fern-like structures slowed down the rate at which they propagated in the regions separating several cavities and the visual effect was a growth pattern which moved toward the periphery of the disk. There was then a period of coalescence, the many cavities merging into one well-defined circular cavity as shown in Fig. 2. Although many filaments of the liquid remained in this region, their static nature would indicate the existence of a constant pressure within the area. It was not possible to determine whether these filaments of residual fluid were clinging to the optical flat or if they extended between the two surfaces. A further separation of the surfaces caused the cavity to collapse. This was an extremely stable phenomenon, the receding boundary wiping out the residual fluid filaments and circular symmetry being maintained until the collapse phase was complete.

The analytical work was based upon the assumptions of (i) laminar flow, (ii) constant viscosity, (iii) an incompressible fluid, (iv) no slip at the solid-liquid boundary, (v) a film thickness h smaller than other dimensions of the system, (vi) a negligible effect of inertia terms, surface tension, and residual fluid in the cavity, and (vii) the cavity boundary being a single circle concentric with the disk. Although the last assumption is not in accord with the observed initial growth pattern, it is realistic for the later stages of the cavity growth. The restrictions of assumption vi can be removed and first-order approximations to the effects of inertia and surface tension can be included without any mathematical hardships. Because of the relative slowness of this cavity formation, in contrast to cavitation phenomena which may be measured in milliseconds, the effect of fluid inertia does not appreciably alter the calculated results. With thin film approximations, a first-order differential equation was obtained for the time rate of change of the cavity radius B, as a function of the disk radius R, the viscosity μ, the film thickness h, the atmospheric pressure p_a, and the cavity pressure p_v:

$$\dot{B} = \frac{h^2}{12\,\mu\,B\,ln\,(B/R)} \times$$
$$\left[P_a - P_v - \frac{3\,\mu\,\dot{h}}{h^3}\,(R^2 - B^2)\right] - \frac{\dot{h}\,B}{2h}$$

By using the recorded data for h and starting the numerical integration of the differential equation at a time when a small cavity was observed experimentally, a theoretical cavity was ob-
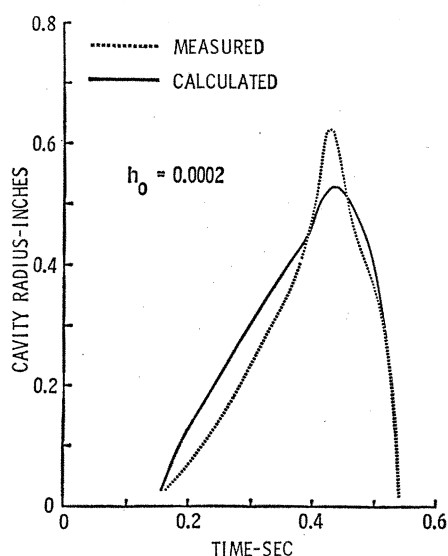
Fig. 3. A comparison between the measured and the calculated cavity radius.

tained which is compared with the observed cavity in Fig. 3. The measured curve for the early stages of cavity growth is based upon an equivalent circular area and, as expected, does not follow too closely the calculated curve. However, for the period where the experimental cavity is circular and assumption vii is fulfilled, there is excellent correlation between measured and calculated values.

DONALD F. HAYS
JAMES B. FEITEN
General Motors Research
Laboratories, Warren, Michigan

Note

1. The proceedings of the symposium are to be published by the Elsevier Publishing Co.
10 June 1963

Magnetite: Preferred Orientation on the Basal Plane of Partially Reduced Hematite

Abstract. *Crystallites of two different orientations have been observed in the polycrystalline magnetite layer formed by carbon monoxide reduction on the basal plane of a hematite single crystal. The relative reducibility of hematite and magnetite ores may be related to this double orientation.*

Blackman and Kaye (*1*), in an electron diffraction study of partially reduced single crystals of hematite (α-Fe_2O_3), found preferred orientation in the surface layer of polycrystalline magnetite (Fe_3O_4) which was formed on the hematite basal plane. Their reduc-

tions were carried out by thermal dissociation at 700° and 1000°C. The orientation reported by them is: (111) magnetite parallel to (00·1) hematite, and [1$\bar{1}$0] magnetite parallel to [1$\bar{1}$0] hematite (*2*).

This orientation would result from a topochemical reaction which maintains the close-packed oxygen layers in the magnetite crystals parallel to those in the hematite crystal. It also agrees with observations of preferred orientation in hematite formed by the oxidation of magnetite (*3*).

In our work, single crystals of hematite (*4*) were reduced by two different methods. In the first of these, a crystal was heated in air at a pressure of 2×10^{-3} mm-Hg and a temperature of 1200°C for 1 minute. The resulting magnetite layer was 1 to 3 μ thick. In the second method, a crystal was reduced in a mixture of 30-percent CO, and 70-percent CO_2 at 1 atm and 657°C for 1 minute. The magnetite layer was 12 to 15 μ thick.

Back-reflection x-ray diffraction patterns from the basal planes of the crystals were recorded photographically with radiation from a cobalt-target tube. These patterns consisted of a superposition of the Laue pattern of the hematite crystal and a portion of the Debye-Scherrer pattern of the magnetite layer. The indexes of the three observed rings in the Debye-Scherrer pattern were 555, 662, and 840. These rings showed the nonuniform intensity distribution about their circumferences that is typically associated with preferred orientation. From an analysis (*5*) of the intensity distribution within the 840 ring as a function of the angle between the normal to the basal plane and the direction of the incident x-ray beam, a (210) pole figure was plotted for each crystal. The pole figure for the crystal reduced by thermal dissociation is shown in Fig. 1. The six symmetrically related areas of high-pole density arise from the orientation reported by Blackman and Kaye (orientation I). The pole figure for the crystal reduced in the CO atmosphere is shown in Fig. 2. The six areas of high-pole density resulting from orientation I are repeated here and, in addition, subsidiary maxima surround each of these principal high density regions. These subsidiary maxima arise from a second, less prominent orientation (orientation II) in which (211) magnetite is parallel to (00·1) hematite, and [$\bar{1}$11] magnetite is parallel to [010] or [0$\bar{1}$0] hematite.
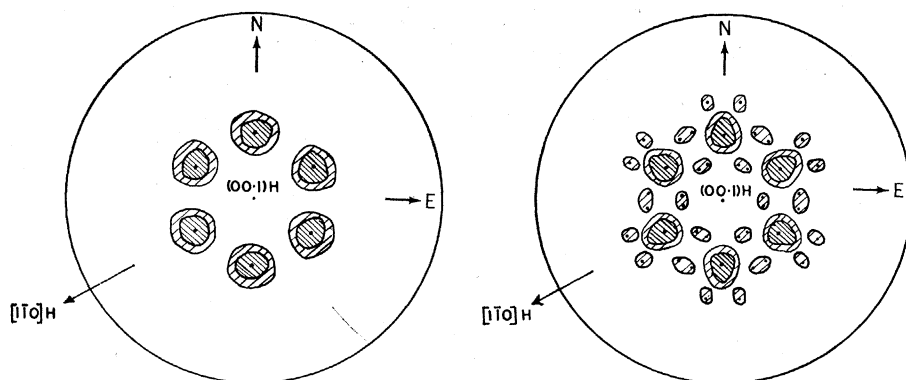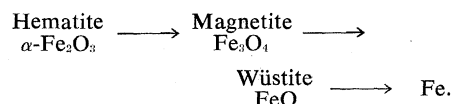
Fig. 1 (left). (210) Pole figure of magnetite on the basal plane of hematite reduced by thermal dissociation. Points represent ideal (210) pole positions. The actual measurements in both figures were limited to the area bounded by the longitudes 72°W and 18°E and by the latitudes 50°N and 34°S. The remainder of each figure was constructed from symmetry. Fig. 2 (right). (210) Pole figure of magnetite on the basal plane of hematite reduced by carbon monoxide. Points represent ideal (210) pole positions. See legend to Fig. 1.

In orientation II, the close-packed oxygen layers of magnetite are thought to be derived from highly distorted versions of close-packed oxygen layers which are perpendicular to the directions [100], [010], and [$1\bar{1}0$] in hematite.

We believe that the double orientation observed on the second crystal has an important bearing on the kinetics of the reduction of iron oxide ores to metallic iron. Starting with hematite, the steps in the reduction, for temperatures above 570°C, are:

$$\text{Hematite} \atop \alpha\text{-Fe}_2\text{O}_3 \longrightarrow \text{Magnetite} \atop \text{Fe}_3\text{O}_4 \longrightarrow$$
$$\text{Wüstite} \atop \text{FeO} \longrightarrow \text{Fe.}$$

Since, compared to hematite, magnetite is already partially reduced, it is somewhat surprising that hematite ores generally become reduced to metallic iron more rapidly than magnetic ores. Bitsianes and Joseph (6), in commenting on this apparent contradiction, have pointed out, among other possible factors, the importance of "grain refinement" (grain size diminution) which accompanies the conversion of hematite to magnetite. According to them, grain refinement would be enhanced by the relatively drastic rearrangement in the crystal structure that must take place in the transition from the hexagonally close-packed oxygen arrangement in hematite to the cubic close-packed arrangement in magnetite. There would, of course, be a similar mechanism operating during the conversion of magnetite to wüstite. However, since the wüstite structure is also based on a cubic close-packed oxygen framework, the rearrangement in the crystal struc-

ture is not so drastic and the degree of grain refinement would be expected to be much less. The larger surface area accompanying grain refinement increases the overall reaction rate by increasing the frequency factor in the Arrhenius expression.

The two orientations of magnetite reported here provide a definite mechanism for grain refinement. Neighboring magnetite crystallites growing in different orientations would meet and be mutually terminated over structurally incompatible surfaces. On the other hand, if only one orientation were possible, neighboring crystallites could join over compatible surfaces and grow into a single larger crystal.

We cannot say that our failure to observe orientation II in the crystal reduced by thermal dissociation is proof that the double orientation does not exist in this case. The very thin layer of magnetite may simply contain too little of orientation II to be observed (7).

ROLLAND O. KEELING, JR.
Department of Physics
DEANE A. WICK*
Department of Metallurgical Engineering, Michigan College of Mining and Technology, Houghton

References and Notes

1. M. Blackman and G. Kaye, *Proc. Phys. Soc. London* 75, 364 (1960).
2. The structure of hematite is referred to hexagonal axes in this paper. The direction [uvw] in the hexagonal system is the direction of the vector $u\vec{a}_1 + v\vec{a}_2 + w\vec{c}$.
3. J. W. Gruner, *Econ. Geol.* 21, 375 (1926).
4. The crystals were from the O'Keefe Lake area, Quebec.
5. See for example: H. S. Peiser, H. P. Rooksby, A. J. C. Wilson, *X-ray Diffraction by Polycrystalline Materials* (Institute of Physics, London, 1955), chap. 21.
6. G. Bitsianes and T. L. Joseph, *Trans. AIME* 203, 639 (1955).
7. Supported by the Institute of Mineral Research at the Michigan College of Mining and Technology. We thank M. E. Volin, director of the institute, for acquainting us with this problem and for his aid and advice. We thank W. A. Hocking for carrying out the reductions and for many valuable suggestions.
* Present address: General Electric Company, Metallurgical Products Department, Box 237, General Post Office, Detroit 32, Mich.

5 July 1963

Low-Latitude Noctilucent Cloud of 15 June 1963

Abstract. A bright noctilucent cloud was observed and photographed northwest of Tucson on 15 June 1963. Results of computations indicate that the cloud was at a height of 71 kilometers. The cloud appears to have resulted from the launching of a Scout space vehicle.

Sun-illuminated clouds have reportedly been seen near the end of twilight in the northwesterly direction from Tucson, Arizona, upon a number of occasions and by numerous persons, including the authors. In particular, the ring-shaped cloud reported by McDonald (1) has been the most spectacular of the group up to date. Since the term "noctilucent cloud" has evolved to refer to a rare type of natural cloud observed only at high latitudes, we wish to extend the use of this term to any cloud that remains illuminated by the sun near the end of astronomical twilight, regardless of latitude or possible origin of the cloud.

On the evening of 15 June 1963, another unusually bright noctilucent cloud appeared in the northwestern sky (Figs. 1 and 2). The cloud persisted in full sunlight until 8:37 P.M. Mountain Standard Time (M.S.T.) and was fully occulted by sunset at 8:51 ± 0.5 minutes M.S.T. as noted by Middlehurst. The correction to local time to give mean solar time is +24 minutes at Tucson and the equation of time is negligible on 15 June so that the meridian passage of the center of the sun's disk occurred at 12:24 M.S.T. The angle to the cloud above the horizon at occultation was 4.5 degrees apparent angle. These parameters, after correction for refraction by the terrestrial atmosphere, yield a height of 71 km (44 miles) for the cloud and a range of 555 km (345 miles) in a direction 40 degrees north of west from Tucson. The location of the cloud is shown in